Journal of Geosciences, 57 (2012), 87–103 DOI: 10.3190/jgeosci.117

Original paper

Structural evolution of the Roudný gold deposit, Bohemian Massif: a combination of paleostress analysis and review of historical documents

Jiří ZACHARIÁŠ*, Zdeněk HÜBST

Institute of Geochemistry, Mineralogy and Mineral Resources, Faculty of Science, Charles University in Prague, Albertov 6, 128 43 Prague 2, Czech Republic; jiri.zacharias@natur.cuni.cz

* *Corresponding author*

The Roudný gold deposit, hosted by a large-scale NNE–SSW trending fault zone (the Blanice Graben), represents a type locality of low-fineness gold (Au–Ag) mineralization in the Bohemian Massif. In order to decipher its structural evolution, we performed a detailed analysis of brittle to brittle–ductile structures on outcrops and of structures described in unpublished historical materials. Three stress phases were distinguished: compressional, strike-slip, and extensional. Most hydrothermal veins originated during the strike-slip and extensional phases. Based on a comparison with the nearby Ratibořské Hory–Stará Vožice deposit, a representative of Ag–Pb–Zn vein type mineralization in the Blanice Graben, we conclude that the structural pattern of both ore deposits/mineralizations (Ag–Pb–Zn and Au–Ag) is compatible with the overall sinistral strike-slip evolution of the Blanice Graben (*c.* 280–270 Ma). Whereas most of the Ag–Pb–Zn veins represent typical extension veins/fractures, early gold-bearing quartz veins of the Roudný deposit were probably initiated as Riedel R' shears and were later reopened during the extensional phase.

Keywords: strike-slip fault, paleostress analysis, hydrothermal ore deposits, gold, Moldanubian Zone, Blanice Graben
Received: 14 March 2012; accepted: 13 June 2012; handling editor: J. Žák

1. Introduction

On a regional scale, orogenic gold deposits (e.g. Goldfarb et al. 2001) tend to occur in the vicinity of large transcrustal "first-order" regional faults and shear zones that served as major conduits for mineralizing fluids (e.g. Cox 1999). On a deposit-scale, however, the ore-shoots are frequently localized within "second- and third-order" structures (e.g. Bierlein and Crowe 2000). The form of veins/mineralization depends on many parameters, especially on the host-rock lithology and rheology, fluid pressure, tectonic stresses, and pressure–temperature conditions of ore formation (e.g. Hodgson 1989; Sibson 2000; Blenkinsop 2008; Micklethwaite et al. 2010).

Two mineralogically and geochemically distinct types of orogenic gold vein-type mineralization have been distinguished in the Bohemian Massif: high-fineness gold (> 90 at. % Au) and low-fineness gold (50–70 at. % Au). Besides gold fineness and mineralogy (e.g. Bernard 1991; Zachariáš et al. 2009) they differ significantly in age and tectonic setting. The high-fineness gold deposits formed at 348–338 Ma (Zachariáš and Stein 2001; Zachariáš et al. 2001) in a transpression zone along a continental magmatic arc represented by granitoids of the Central Bohemian Plutonic Complex (Žák J et al. 2005, 2012). In contrast, the low-fineness gold deposits are considerably younger (*c.* 300 to 280 Ma; no geochronological data exist) and related to late-Variscan mostly brittle fault zones (e.g. the Blanice Graben) in the Moldanubian Unit. The presence of lower-temperature hydrothermal alterations (sericitization, kaolinization) and dominance of brittle structures makes the low-fineness gold deposits very similar to "300 Ma" gold-deposits of the Massif Central in France (e.g. Bouchot et al. 1997).

The structural evolution of low-fineness gold deposits, as well as of the Blanice Graben, is poorly constrained. This article aims to fill this gap by a study of the Roudný gold deposit (a type locality for the low-fineness Au mineralization in the Bohemian Massif; e.g. Bernard 1991). Unfortunately, access to the underground parts of the Roudný mine is impossible at present. Therefore, here we attempt to extract valuable geological information from the available historical documents, combining and comparing these data with our own analysis of brittle and ductile structures on outcrops. However, this study is not intended to serve as an exhaustive review of historical documents or mining activities at Roudný. For this purpose, the reader is referred to excellent compilation of Zemek (2001), or older reviews by Slavík (1912), Šusta (1922), Hála (1923), Ježek (1930, 1931), and Ježek and Hoffmann (1933).

2. Brief history of the Roudný mine

Gold mining at Roudný dates back to the 14th century, or perhaps even earlier. Limited small-scale mining was also performed by the Auersperg family between 1769 and 1804. Modern exploitation of the deposit was connected with the famous Czech geologist F. Pošepný (1836–1895), who rediscovered historical documents regarding the past mining at Roudný and identified traces left by these activities in the field. His findings motivated M. Becker of the German Stantien & Becker Co. to invest into reopening the Roudný mine on May 1st 1893. However, mining was not intensive and well managed and was abandoned in 1901. A new mine owner, the English Sugdan & Fischer Co., reopened the mine on September 10th 1904 and, over a short period, Roudný became one of the most modern gold mines in Europe, supplying approximately 80 % of the gold in the Austro–Hungarian Empire. Unfortunately, irregular gold distribution, variable ore grade, and the World War I brought the mine into decline. Mining was finally terminated in 1930/1931. According to Morávek et al. (1992), 5770 kg of gold was mined from the deposit between 1904 and 1930. The total amount of extracted gold, including mining in the Middle Ages, is estimated at 6770 kg. The average fineness of the recovered gold in the period of 1896–1930 was 650–667/1000; the average ore grade was 10.5 g/t Au.

Exploration activities at Roudný were renewed during the World War II and then continued from 1945 till 1956. During the later period the mine was deepened to a level of –520 m and new gold reserves were calculated. The Czechoslovak state exploration company Geoindustria re-evaluated the gold reserves at the upper mine levels (0–200 m) and in abandoned tailings (~800 kg of gold at 2 g/t Au in tailings; Švestka and Hron 1993) in 1987–1990. They also performed some limited exploration activities, mainly in the area NE of Roudný; however, no economically viable continuations of the electrum mineralization were found in or near the Roudný mine (Komínek et al. 1990).

3. Regional geology

The Roudný deposit is hosted by the Moldanubian Unit (Fig. 1), which represents an intensively metamorphosed crystalline complex with three lithotectonic units: Ostrong (Monotonous), Drosendorf (Variegated), and Gföhl (e.g., Fiala 1995; Franke 2000). The Ostrong Unit is dominated by paragneisses, whereas the Drosendorf Unit also contains quartzites, marbles, orthogneisses, amphibolites, and graphitic schists. They both were metamorphosed under amphibolite-facies conditions.

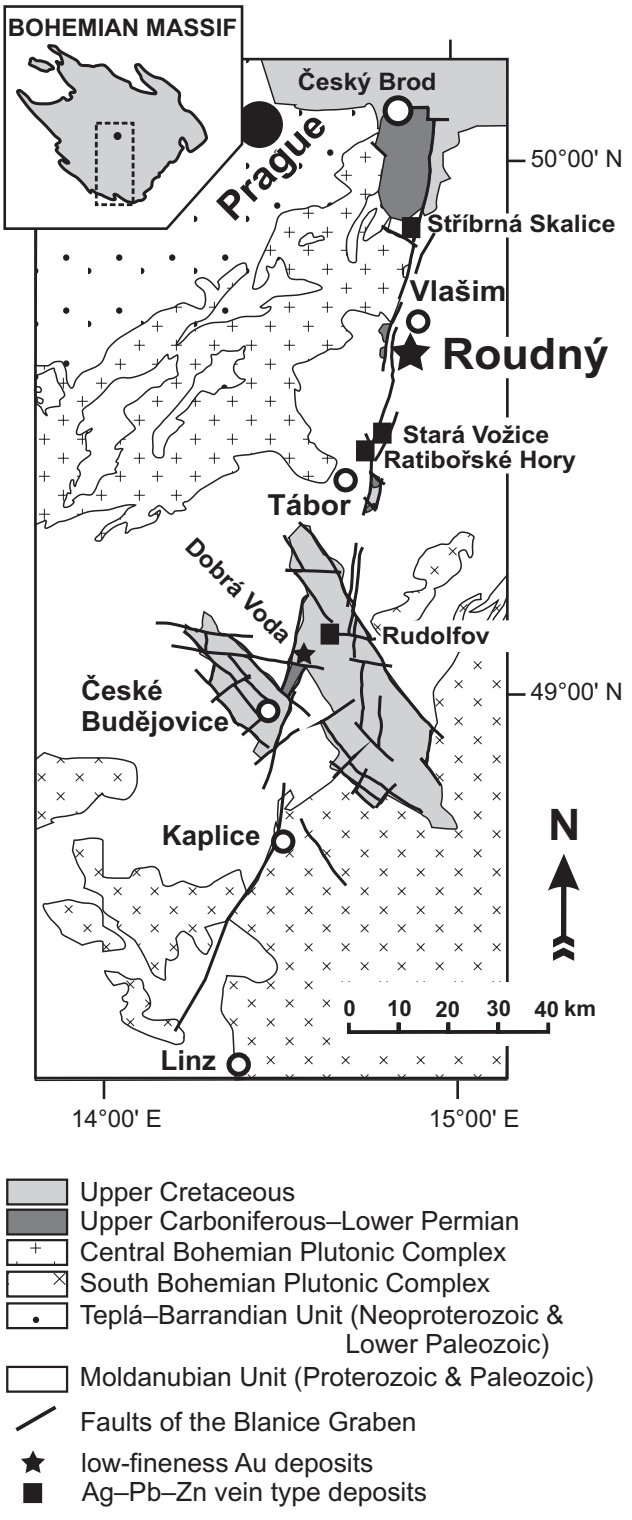

Fig. 1 Simplified geological map of the Blanice Graben and surrounding units with locations of the Ag–Pb–Zn and Au vein-type ore deposits.

Prominent rocks of the Gföhl Unit represent granulites with orthogneisses accompanied by minor eclogites and peridotites. They record the granulite- to eclogite-facies

conditions at about 340 Ma (e.g. Faryad et al. 2010; Friedl et al. 2011). The Moldanubian Unit was intruded by two large Variscan plutonic complexes: the Central Bohemian Plutonic Complex (CBPC; e.g. Janoušek et al. 1995; Holub et al. 1997b) and the Moldanubian Plutonic Complex (MPC; e.g., Breiter and Sokol 1997; Breiter 2001). The CBPC consists of five to seven magmatic suites (predominantly I-types, I/S-types and rare S-types), with the intrusion ages varying from 354 ± 4 to 337 ± 1 Ma (e.g. Holub et al. 1997a; Žák K et al. 1998; Janoušek and Gerdes 2003; Janoušek et al. 2004, 2010; Dörr and Zulauf 2010). The MPC consists of three to four principal intrusive groups (mostly S and S/I types, rarely I-types; Holub et al. 1995; Klečka and Matějka 1996; Matějka and Janoušek 1998), ranging in age from 330–323 Ma to 305–302 Ma (see Bankwitz et al. 2004 for review).

The Roudný deposit is located in the northern part of a crustal-scale brittle tectonic zone of the Blanice Graben east of the CBPC (Fig. 1). This NNE–SSW trending, approximately 200 km-long zone (also called the Kouřim – Blanice – Kaplice – Rödl fault zone) cuts across all the Moldanubian lithotectonic units and extends from east of Prague to Linz in Austria. The faults of the Blanice Graben have been repeatedly reactivated; the oldest identified tectonic activity was of the Permo–Carboniferous age (Stephanian C to Autunian; Holub 2001) as inferred from coal-bearing sediments occurring in several isolated depocenters. The major tectonic movements along the Blanice Graben must, therefore, have been Permian or younger. The only geochronological data on the tectonic evolution of the Czech part of the Blanice Graben are those of Košler et al. (2001) and Vrána et al. (2005). The former authors studied a microgranodiorite dike that cuts through the Moldanubian paragneisses in the vicinity of a major NNE–SSW fault of the Blanice Graben. They suggested (1) a minimum intrusive age of 270 ± 2 Ma ($^{40}Ar/^{39}Ar$ on hornblende) for the microgranodiorite dike swarm, (2) magma origin by re-melting of the lower crust with a possible component from upper mantle, (3) spatial and temporal association of dike emplacement with the fault movements along the Blanice Graben, and (4) a temperature of less than 200 °C for the surrounding Moldanubian host rocks at the time of the dike emplacement. Vrána et al. (2005) obtained cooling age of 303 ± 5 Ma on a hornblende from a 0.5 m wide dike of quartz diorite porphyry near Kaplice (Fig. 1). This dike is spatially and genetically associated with NNE–SSW trending swarm of biotite granodiorite porphyries closely tied to the Kaplice–Rödl fault zone, and intrusion of the dike postdated the ductile deformation in this fault zone. Vrána and Bártek (2005) inferred the sinistral displacement of about 17 km along the Kaplice–Rödl fault zone in this area.

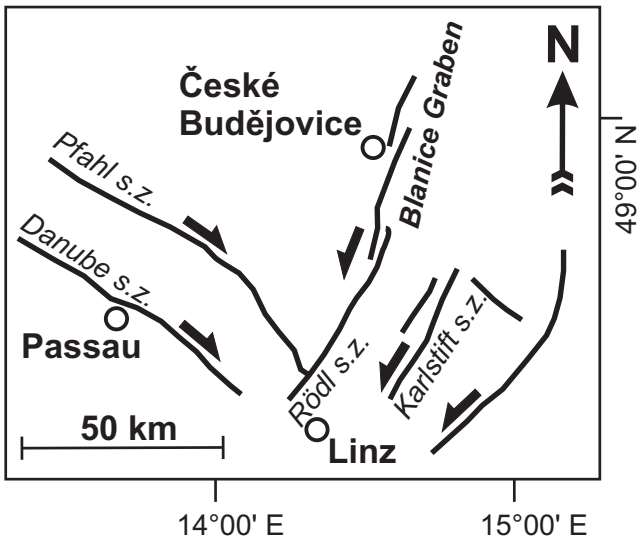

Fig. 2 Scheme of ductile and fault shear zones in the southern part of the Bohemian Massif (after Brandmayr et al. 1995). Conjugated pattern of dextral and sinistral shear zones resulted from a strike-slip regime with N–S oriented compression and E–W oriented extension. According to this scheme the studied Blanice Graben is a sinistral strike-slip fault zone.

The southernmost (Austrian) part of the Blanice Graben (also referred to as the Kaplice–Rödl fault zone or the Rödl shear zone) is a sinistral ductile shear zone with pronounced subhorizontal stretching lineation. Synkinematic mylonitization along this zone was dated at around 288–281 Ma (Brandmayr et al. 1995; Ar–Ar method on muscovite). Based on these authors, the Blanice Graben is a part of conjugated strike-slip ductile and fault system (Fig. 2), consisting of dextral (NW–SE) and sinistral (NE–SW) shear/fault zones originated under N–S oriented compression and E–W oriented extension.

The Blanice Graben hosts numerous minor hydrothermal ore deposits. Low-fineness Au mineralization is represented by the Roudný type locality and by another small historical district (Dobrá Voda near České Budějovice). The mineralization is characterized by gold with significant admixture of Ag (electrum; 40–30 wt. %), the abundance of sulfides (pyrite and arsenopyrite), and extensive hydrothermal alterations (kaolinization, sericitization and pyritization). The absence of molybdenite, scheelite/wolframite, and Bi–Te–(S) phases represents another significant diagnostic feature.

The Ag–Pb–Zn, mostly vein-type, mineralization (e.g. Stříbrná Skalice, Ratibořské Hory–Stará Vožice, Rudolfov) is younger than the low-fineness Au mineralization. It is characterized by quartz–carbonate gangue, abundant galena accompanied by sphalerite and Ag-phases (miargyrite, pyrrargyrite, argentite, and native silver), and by the scarcity of Fe-sulfides (pyrite, arsenopyrite and pyr-

rhotite). Individual deposits were mined intermittently from the 14th to the 17th century; most of the Ag-rich parts were usually referred to as the cementation zones (i.e. enriched by supergene processes).

4. Geology and mineralogy of the deposit

The Roudný deposit is hosted mainly by the sillimanite–biotite and biotite paragneisses of the Drosendorf Unit. The biotite gneisses contain small but numerous intercalations of quartz-rich gneisses and quartzite occurring in bands about 5 to 20 cm thick. Intercalations of skarn, amphibolite, and calc-silicate rocks are rare. The gneisses are intruded by numerous small aplite dikes and pegmatite bodies (Fig. 3a).

The Roudný ore body fills in an irregular "triangular prism to cone-like" body (Fig. 3b; with an axis inclined at an angle of approximately 50–60° to the WNW), delimitated by intersection of three to four brittle faults (Fig. 3a): the Hangingwall, the Footwall, the Michal (Michael) and the Pavlína (Paulina) faults. The main part of the ore body consists of a single quartz vein ("Main Vein") and associated irregular quartz stockwork and minor sulfidic impregnation in the altered rocks (Figs 4–5). According to Ježek (1930) the "Main Vein" strikes parallel to the Hangingwall Fault, it is 10 to 150 cm thick (most frequently only 30–50 cm) and locally splits into several subparallel veins. The quartz stockwork is developed mainly in the gneisses and, to a lesser extent, in the aplites and pegmatites but never in the calc-silicate rocks (Šusta 1922). The horizontal length of the Roudný ore body along its strike varies between 75 and 130 m, with a thickness of 4–6 m.

Atypical N–S trending Au-bearing quartz–aplite vein with disseminated pyrite and arsenopyrite was discovered at level –170 m (Hradecký 1911a) *c.* 200 m west of the Pavlína Fault (i.e. outside the triangle). The vein is about 7 m thick, dips 45° to the W (same dip as the Pavlína Fault) and is displaced by the Hangingwall Fault (see map on page 170 of Hradecký 1911b).

The Michal Fault strikes mostly E–W and is considered to be youngest. It displaces the Pavlína Fault

⇨

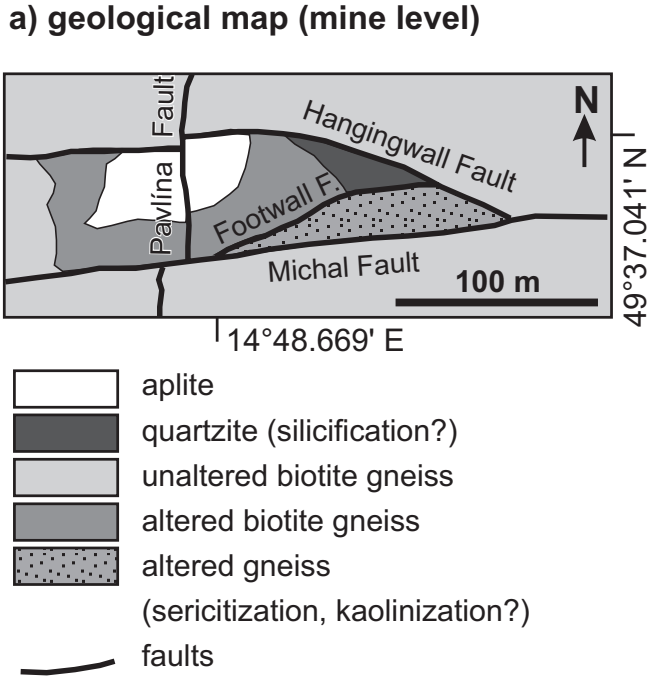

Fig. 3a – Schematic geological map of an unspecified level (probably around –200 m) of the Roudný mine (modified after Hradecký 1911b). **b** – Pseudo-3D projection of the Roudný ore body (highlighted in grey). Ore body represented by the "Main Vein" and irregular quartz stockwork are mostly located within a triangular prism delimited by the intersection of three (four) subvertical faults. Fault intersections with the horizontal planes of the mine levels are schematically shown by thick lines (modified after Ježek and Hoffmann 1933). **c** – Projection of mined ore blocks from individual mine levels of the Roudný mine onto a single horizontal plane. The long dotted line labeled by its azimuth marks trend from shallow to deep mine levels (i.e. trend of the ore body axis).

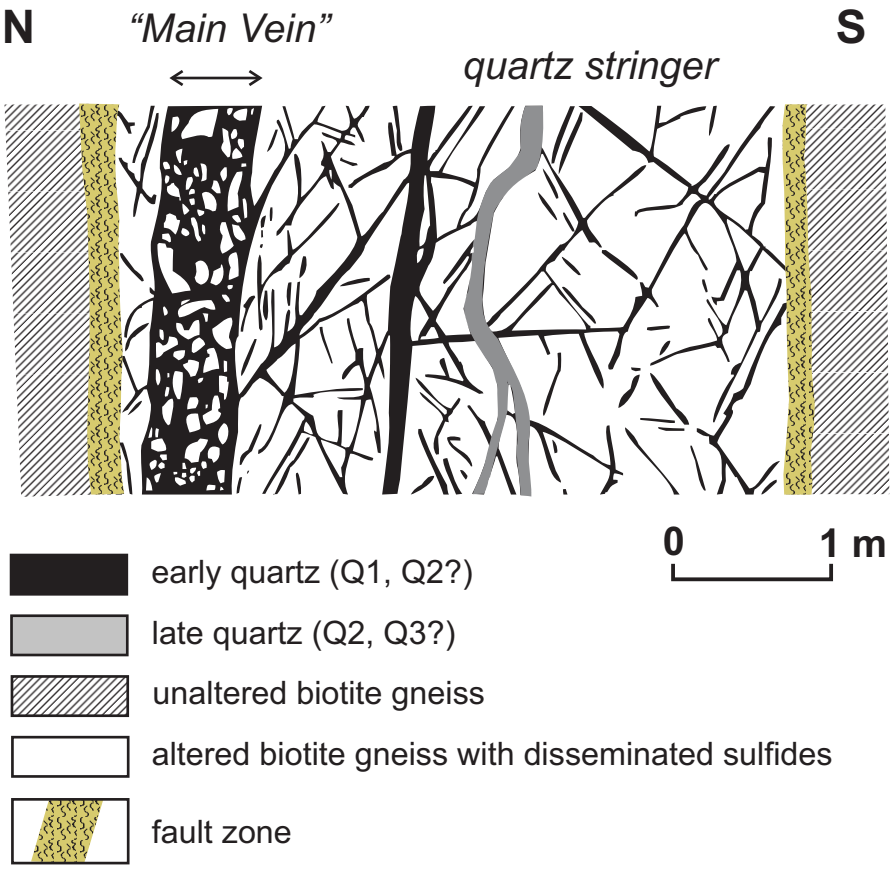

Fig. 4 Vertical cross section across the ore zone with identification of the "Main Vein" (thick black vein with breccia texture; Q1 in our classification), of an irregular quartz stringer (thin black veinlets; probably also Q1, or Q2) and of a late quartz vein crosscutting the stringer. The nature of this late vein (Q2 or Q3) is difficult to assess. The contact of the ore zone with the surrounding gneisses is tectonic. Note the steep dip of the "Main Vein". Modified after Šusta 1922 (fig. 3).

by 12 m (at the –170 m level), as well as all the other faults (Fig. 5). The Pavlína Fault zone strikes N–S and is the second youngest fault. At shallow levels (–120 to –230 m) it is represented by two subparallel faults and, at deeper levels, by only a single one. In almost all the maps, the Pavlína Fault displaces both the Hangingwall and the Footwall faults. The Footwall Fault is usually considered to be the oldest (e.g. Šusta 1922; Ježek 1930; Ježek and Hoffmann 1933). Some faults exhibit gradual changes in fault strikes with increasing depth (Fig. 5): at shallow levels, the Michal Fault strikes E–W and all the faults delineate well a triangular body. With increasing depth, the Hangingwall and the Michal faults become dominant and more or less subparallel (WNW–ESE at –480 m level).

Mineral paragenesis of the deposit was summarized by Novák (1956). He distinguished three main mineralization stages that included four generations of quartz, two generations of gold, and five generations of pyrite. His scheme was adopted and slightly modified by Paterová (2001) with Zachariáš et al. (2004, 2009). A detailed study of individual pyrite and arsenopyrite generations as well as discussion of arsenic and gold substitution in pyrite/arsenopyrite can be found in Zachariáš et al. (2004).

For the purpose of the current study, we use the following gangue subdivision:

Early quartz (Q0): the oldest generation of hydrothermal quartz accompanied by tourmaline (schorl). It may be difficult to distinguish it from veins of metamorphic segregation quartz or from quartz lenses associated with the tourmaline-bearing pegmatite/aplite dikes/bodies.

Main quartz (Q1): the next quartz generation represented by massive milky quartz that fills in major veins (several cm up to several meters thick) in the deposit. In historical documents, this quartz was referred to as the "Main Vein" (Fig. 4).

Main ore quartz (Q2): dark to light grayish massive quartz rich in disseminated sulfides (arsenopyrite, pyrite) usually filling in fractures (breccia zones) in the massive milky quartz (Q1), or forming individual veinlets and impregnations in the altered host rock.

Late ore quartz (Q3): forming numerous thin veins (up to 1 cm thick), frequently exhibiting bilateral symmetry and locally drusy texture.

The thin carbonate and fluorite veins are younger than most of the late quartz veins (Q3). Carbonates also fill in some segments of the brittle fault zones.

5. Relationships between mineralization and faulting

When mining started, the ore body was considered to be hosted exclusively within the "fault triangle/cone". The "Main Vein" was supposed to be older than the faults and displaced by them. As mine activities proceeded, it was documented at several places that the gold-ore zones also extend beyond the "fault triangle" (Ježek 1930; Urban 1956, 1957; Kovald 1951). Most of the Au-mineralization is thus younger than the major displacements along the main faults. Zoubek (1945) and other authors

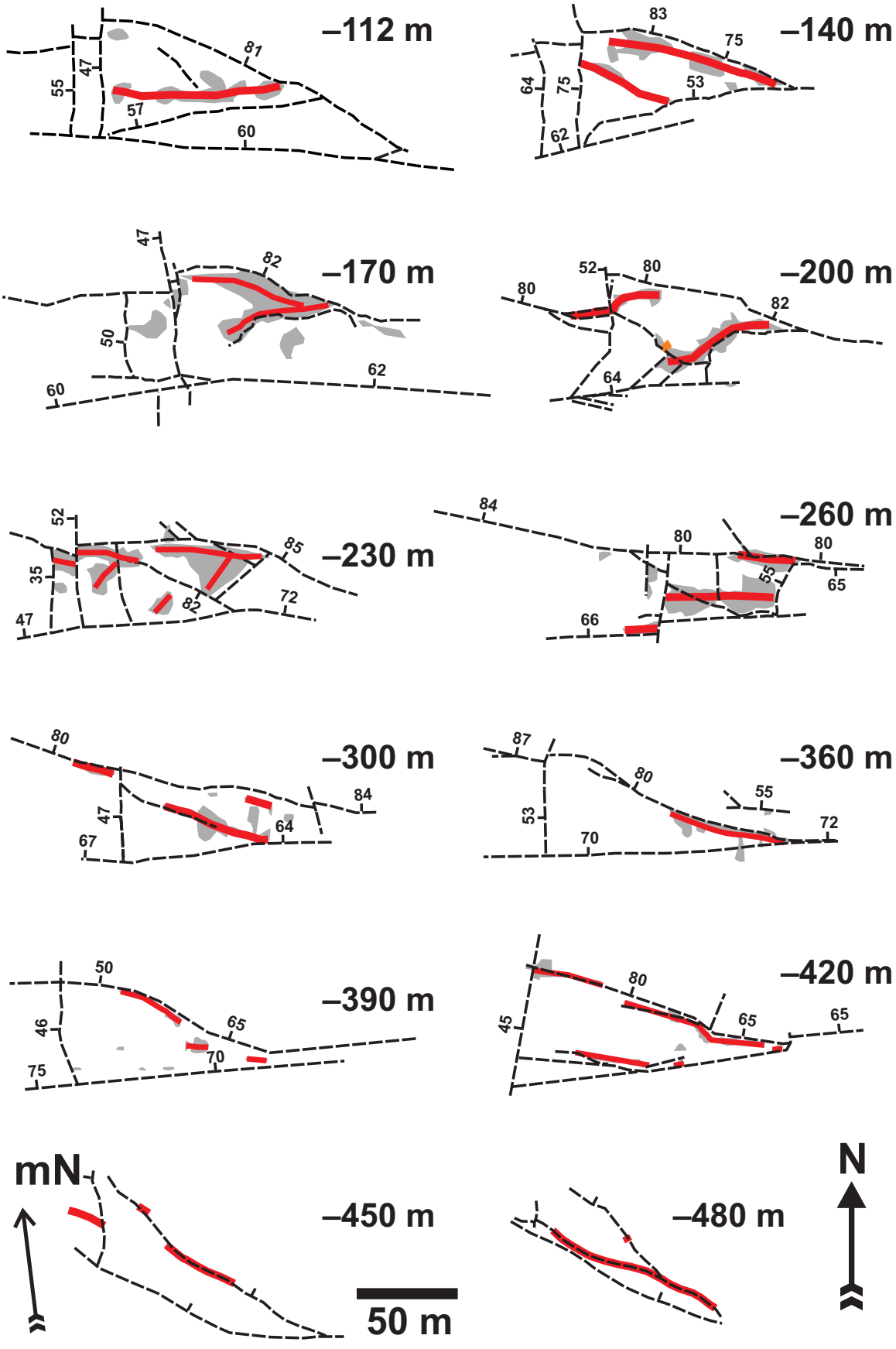
–112 m
81
47
55
57
60
–140 m
83
75
64
75
53
62
–170 m
47
82
50
62
60
–200 m
52
80
80
82
64
–230 m
52
85
35
82
72
47
–260 m
84
80
80
55
65
66
–300 m
80
84
47
64
67
–360 m
87
80
55
53
72
70
–390 m
50
46
65
70
75
–420 m
80
45
65
65
mN
–450 m
50 m
–480 m
N

(Malachov 1954; Urban 1954; Novák 1956) therefore suggested that the triangular zone delimitated by the intersection of faults (i.e. the ore body) served only as a passive conduit for focused fluid flow.

In contrast, the earlier authors suggested that the "Main Vein" was segmented by one or more of the faults into two or more separate parts. Therefore, early exploration activities focused on finding the missing vein segment. For example, former mine director A. Hoffmann suggested displacement of the missing segment to the west along the Hangingwall Fault. In contrast, Šusta (1922) assumed displacement along the Footwall Fault to the east. However, exploration adits conducted in all the perspective directions (to W, to E and to N) failed to find mineralization similar to the Roudný "Main Vein". This seems to validate the above mentioned conclusion of Zoubek (1945).

Last, Urban (1956) noticed that the Michal Fault at level –450 m forms a sharp boundary between the hydrothermally altered gneisses (inside the mineralized triangle) and the non-altered gneisses (to the south of the fault). This suggests post-mineralization reactivation of the Michal Fault.

6. Historical materials

A large body of structural data was excerpted from historical mine documentation. Unfortunately, not all the structural data were documented with the same care and extent. Therefore, the greatest amount of data is related to faults and metamorphic foliation. Although various quartz veins and pegmatite/aplite dikes were also mapped, their orientation and mineralogy were rarely documented. Historical materials used in this study comprise surface geological maps, mine underground maps and mine vertical cross-sections compiled by geologists and technicians of the former mine office (Hradecký, Sedláček, and Rudie authored many of them). All these documents are stored in the state archives (Geofond, Prague and Kutná Hora) and can also be downloaded from *http://www.geofond.cz/wbanskemapy/*. Detailed schemes and maps of underground faces or galleries, mostly drawn by geologist Josef Vinický during the renewed mine exploration (1953–1957), are also stored at Geofond.

⇦

Fig. 5 Summary of main structures identifiable at individual mine levels (depth is indicated in the upper right corner of each figure). The course of all the faults (thin dashed lines) was redrawn from original maps, while the course of the "Main Vein" (thick solid line) is mostly hypothetical and resulted from interconnecting the individual main mined blocks (shadowed). At some levels (–360 m, –450 m), the exact position of the "Main Vein" was indicated in the original maps.

7. Structural data

In addition to the structural data taken from historical materials, we documented all the existing outcrops in the Roudný area in detail, focusing mainly on the relationships between quartz veins and other brittle and ductile structures, as well as on paleostress analysis of brittle structures. The data were then treated in four separate subsets: surface outcrops above the Roudný mine (referred to as "mine surface"), the underground of the Roudný mine ("mine underground"), the entrance part of the Prokop (Moritz) adit ("Prokop adit"; located 1 km ESE of the mine) and a small area *c.* 1 km S of the mine (called "Vinice").

7.1. Ductile structures and dikes

Metamorphic foliation (S_1) is the most prominent feature in the studied area. It exhibits mostly uniform dip to the N or NW (Fig. 6a). We have identified some limited variations in the S_1 orientation (calculated eigenvectors of S_1 data subsets have orientation: 130°/50° "mine surface", 173°/46° "mine underground", 211°/43° "Prokop adit" and 140°/23° "Vinice").

Stretching lineation (L_1) associated with the S_1 planes generally trends to the NW (Fig. 6b; eigenvector 316°/44°), but it is mostly weak, suggesting generally oblate fabric. In the "Vinice" area, we identified several minor folds (up to 1 m in amplitude) developed in calc-silicate layers in quartzite gneiss. Fold axes (La) show homogeneous orientation and plunge gently to the NNE (Fig. 6b; eigenvector 17°/8°).

According to the historical documents, aplite and pegmatite form numerous small dikes and pockets at Roudný. They are mostly, but not exclusively, parallel/subparallel to the S_1 foliation (Fig. 6c) and less than 10 cm thick. Subvertical dikes (mostly striking ENE–WSW) are also relatively frequent. A few larger aplite bodies were also reported in the mine underground/surface (e.g. Fig. 3a). Their strike, dip and form are, however, difficult to assess. In addition to pegmatites/aplites (often tourmaline-bearing), monomineral tourmaline veins/lenses, up to several centimeters thick and less than 2 m in along-strike length, can be found. They are mostly parallel to the S_1 foliation (Fig. 6c; eigenvector of "mine underground" data has orientation 4°/23°). Steeply dipping tourmaline veins are more common in the vicinity of some fault zones.

7.2. Quartz veins

Despite the existing detailed classification of quartz veins at Roudný (see above), it is quite difficult to distinguish

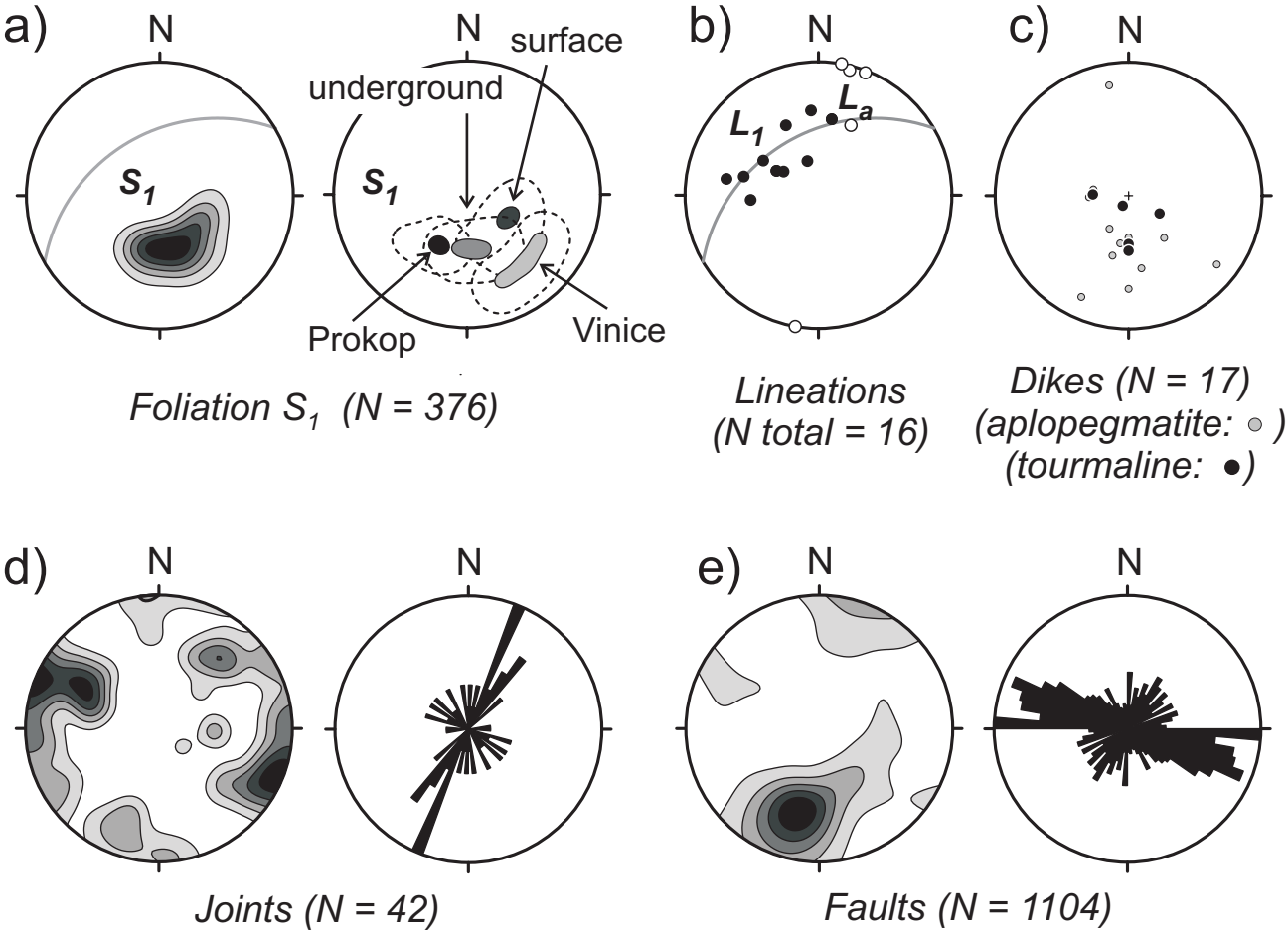

Fig. 6 Summary of structural elements (lower hemisphere equal angle projection or rose diagram) of the Roudný area: **a** – maxima and schematic extent of poles to metamorphic foliation Sl in the four studied areas; **b** – stretching lineation (L_1) from the "mine surface" and fold axes (L_a) at "Vinice"; **c** – poles to aplite/pegmatite dikes/lenses and of tourmaline "veins"; **d** – joints at the "mine surface" (contour diagram of poles and rose diagram of strikes); and **e** – summary of faults at both the mine surface and in mine underground (contour diagram of poles and rose diagram of strikes).

the individual quartz vein types in the available historical documents, where mineralogical details are usually sparse.

Q0: Tourmaline-bearing quartz (Q0) veins/lenses are relatively rare. We have found only one such lens at the "mine surface", being parallel to the S_1 foliation and *c.* 5 cm thick.

Q1: Thick veins consisting of massive milky quartz were denoted as Q1 veins. According to Šusta (1922), the "main quartz vein" at the Roudný deposit consisted mostly of Q1. The "Main Vein" described by Šusta (1922; his Tab. 2) at the mine level of –360 m is a single quartz vein striking 289°, less than 1 m thick, locally split into 2–3 subparallel veins. Other "Main Vein" schemes result in similar strikes of 283° (Šusta 1922, his fig. 7), 290° (unpublished scheme) and 289° (our compilation of mined blocks; Fig. 3c). In all these historical schemes the "Main Vein" is plotted close to the "Hangingwall Fault", running parallel to it. Although the dip of the "Main Vein" was not stated, we can estimate it to vary between 75°–90° to the N to NNE (see Fig. 4). Hradecký (1911a) recorded similar dip values (68°–80° to N).

A slightly different situation can be derived from figure 6 of Šusta (1922). The vein plotted was also referred to as the "Main Vein"; however, it strikes 251° and is located along the "Footwall Fault". The vein itself is less than 0.5 m thick, but the total width of the mined (Au-mineralized) zone is 7–8 m.

Q2: The greyish quartz (rich in disseminated sulphides) was denoted as Q2. We found only two historical drawings that distinguish between various types of quartz gangue (Šusta 1922, his figs 3 and 4; and Fig. 4 herein). The subvertical dip of veins Q1 and Q2 can be depicted on the basis of these drawings; strike (E–W to WNW–ESE) can only be inferred from the assumed perpendicular orientation of the section (N–S).

Q3: Numerous quartz veins typically less than 1 cm thick and frequently of crustiform texture were denoted

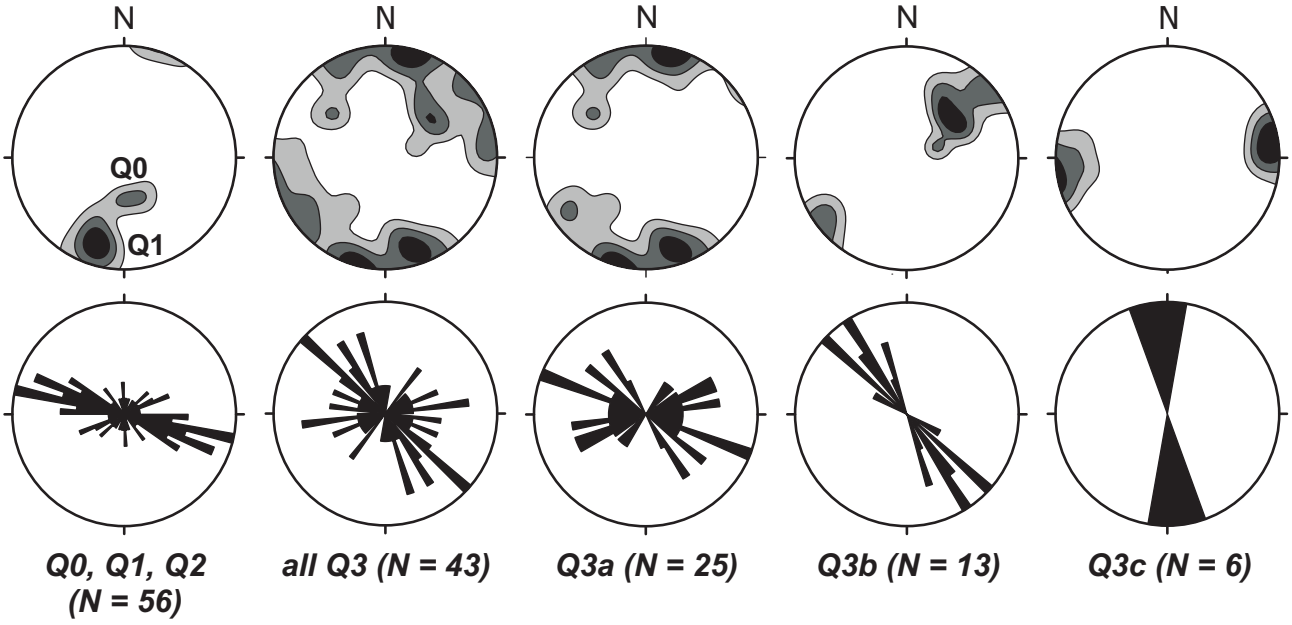

Fig. 7 Summary diagrams of quartz veins orientations (lower sphere equal angle projection of vein poles and rose diagram of vein strikes). Data for most of Q1 and Q2 veins were excerpted from historical documents, while Q3 data were measured at the "mine surface".

as Q3. Due to this texture they can easily be distinguished from Q1 and Q2 in the field. Figure 7 summarizes nearly all the Q3 veins measured at the "mine surface". The Q3 veins vary significantly in strike and dip; the general strike (289°) is, however, similar to that of Q1 veins. In detail, several local density maxima of Q3 poles can be depicted (Fig. 7; 316°/44°, 49°/26° and 264°/2°). They correspond to three successive generations of Q3 veins, referred to as Q3a, Q3b and Q3c, respectively. The Q3c veins are relatively sparse. They are filled in with a mixture of iron oxyhydroxides with minor quartz. Finally, bilaterally symmetrical crustiform vein texture and the absence of any slip component along most of the Q3 veins allow us to consider Q3 veins as extensional.

7.3. Joints and faults

Closely spaced (10–50 cm), steeply dipping joints free of any mineralization measured at the "mine surface" display an orthogonal pattern (Fig. 6d), consisting of dominating NNE–SSW joints and of less abundant E–W joints. In addition to steep orthogonal joints, another set of joints is clustered around 40°/20° (pole maxima). Faults and joints data excerpted from the historical documents ("mine underground") exhibit one marked orientation density maximum at 194°/25°, and another, less significant, at 294°/26°, again with orthogonal symmetry (Fig. 6e).

We have identified a total of 40 fault planes (Fig. 8 and Tab. 1) containing kinematic indicators (slickensides) at "mine surface" outcrops (measured at 19 outcrops).

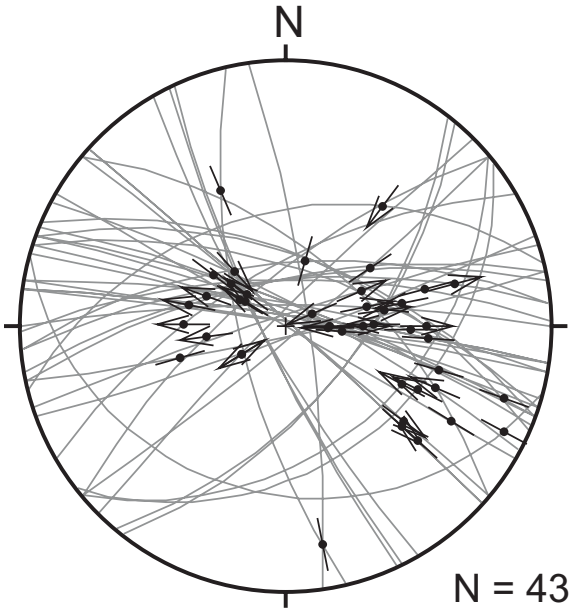

Fig. 8 Complete set of fault-slip data from the Roudný mine (mostly surface outcrops) used in the paleostress analysis.

Another three fault-slip data were excerpted from the historical documents ("mine underground"). Most kinematic indicators are represented by asymmetric elevations, crescentic markings (carrot-shaped plucking markings), and small steps with sharp-borders (e.g. Doblas 1998). Rarely we have found evidence for trailed material. No syntectonic mineral fibers were found.

We suggest that three outcrops (five fault-slip data) from the "mine surface" represent traces of the Michal

Tab. 1 Fault-slip data from the Roudný mine (mostly surface outcrops) used in the paleostress analysis

Nb.: [1]	Reliability[2]	Type [3]	Azimuth[4]	Dip[5]	Rake[6]	Direction[7]	Phase [8]	Nb.: [1]	Reliability[2]	Type [3]	Azimuth[4]	Dip[5]	Rake[6]	Direction[7]	Phase [8]
1	P	N	330	65	55	W	1	23	P	N	42	88	30	E	2
2	*	?	210	90	18	E	1	24	*	?	168	85	45	W	1
3	C	I	315	85	68	W	1	25	P	N	240	80	72	N	2
4	C	N	160	85	68	W	1	26	P	N	245	80	71	W	2
5	P	I	8	88	72	E	1	27	P	I	244	80	60	W	1
6	P	I	346	43	46	E	1	28	P	N	0	81	56	E	2
7	C	I	20	60	50	E	1	29	P	N	8	85	58	E	2
8	C	N	18	65	38	E	2	30	C	N	342	85	55	E	2
9	P	N	130	60	60	N	2	31	*	?	82	80	10	S	1
10	S	I	128	60	68	N	1	32	*	?	140	85	48	E	3
11	*	?	195	25	12	E	1	33	P	N	320	70	62	W	2
12	P	I	140	40	72	E	1	34	S	N	348	70	53	W	1
13	P	I	142	35	68	E	1	35	S	N	350	70	60	W	1
14	*	?	359	70	35	E	1	36	P	I	40	59	32	S	1
15	*	?	10	80	40	E	1	37	*	?	10	88	66	E	1
16	C	N	355	70	25	E	2	38	*	?	355	63	80	E	1
17	*	?	23	60	9	E	1	39	*	?	16	85	72	E	1
18	*	?	22	80	54	W	3	40	*	?	8	85	33	E	1
19	*	?	20	80	62	W	3	41	*	?	18	85	68	W	3
20	P	I	28	80	82	E	1	42	*	?	20	83	28	E	1
21	P	N	40	88	30	E	2	43	*	?	257	70	33	N	1
22	P	I	42	88	23	E	1								

[1] – number of a fault-slip measurements
[2] – reliability of the measurement of the actual direction of slip along the fault (* – the type of the fault is not known; P – probably; S – supposedly; C – certainly).
[3] – type of the fault (N – normal fault; I – reverse fault; S – sinistral fault; D – dextral fault)
[4] – azimuth of the fault-dip
[5] – dip of the fault-dip
[6] – angle between the slickenline on the fault plane and the intersection-line between the fault plane and the horizontal plane (i.e. "rake or pitch")
[7] – geographic direction from which the lineation-inclination (rake) is measured
[8] – separation of fault-slip data into individual tectonic phases (1 – compressional phase, 2 – extensional phase, 3 – excluded)

Fault (fault plane 5°/85° with the northeast- to east-trending slickenlines, 40° to 72°). Šusta (1922) and Ježek (1930) gave similar data for the Hangingwall Fault (fault plane 8°/85° with 33° east-trending slickenline at level –200 m, and fault plane 20°/83° with 28° east-trending slickenline trending at –360 m level, respectively).

Paleostress analysis of veins, dikes and fault-slip data was performed using the numerical Gauss method (Žalohar and Vrabec 2007), the data were processed in the T-Tecto software (version 3.0; author J. Žalohar). In the first step, we suggested a heterogeneous data set and therefore accepted a larger misfit value (50°–60°) between the theoretical and real slip vectors. Then we used lower misfit values (15°–20°) and repeated calculations. Both calculations yielded almost identical results and resulted

⇨

Fig. 9a – Separation of fault-slip data, based on the paleostress inversion analysis using the Gauss method (Žalohar and Vrabec 2007), into compressional and extensional subsets (stress phases). Paleostress axes: σ_1 = large square, σ_2 = medium-sized square and σ_3 = small square; kinematic axes are shown by circles; all stereoplots represent lower hemisphere equal angle projection. Solid arrows indicate orientations of maximum horizontal compression and/or extension. Small stereoplots document confidence of stress tensor (contoured plots) where magnitudes of individual stresses are highlighted by colors (red = maximum compression, blue = minimum compression (maximum extension), green = intermediate stress). Next stereoplots display results of the paleostress analysis using the Right Dihedra method of Angelier and Mechler (1977). The next row of plots shows the confidence of the parameter D estimate and magnitudes of stresses using the Mohr diagram. **b** – Results of paleostress analysis of mode-1 fractures (extensional veins/dikes) using the Gauss function (paleostress axes: σ_1 = large circle, σ_2 = medium-sized circle and σ_3 = small circle; same colors as above) and the data used the analysis.

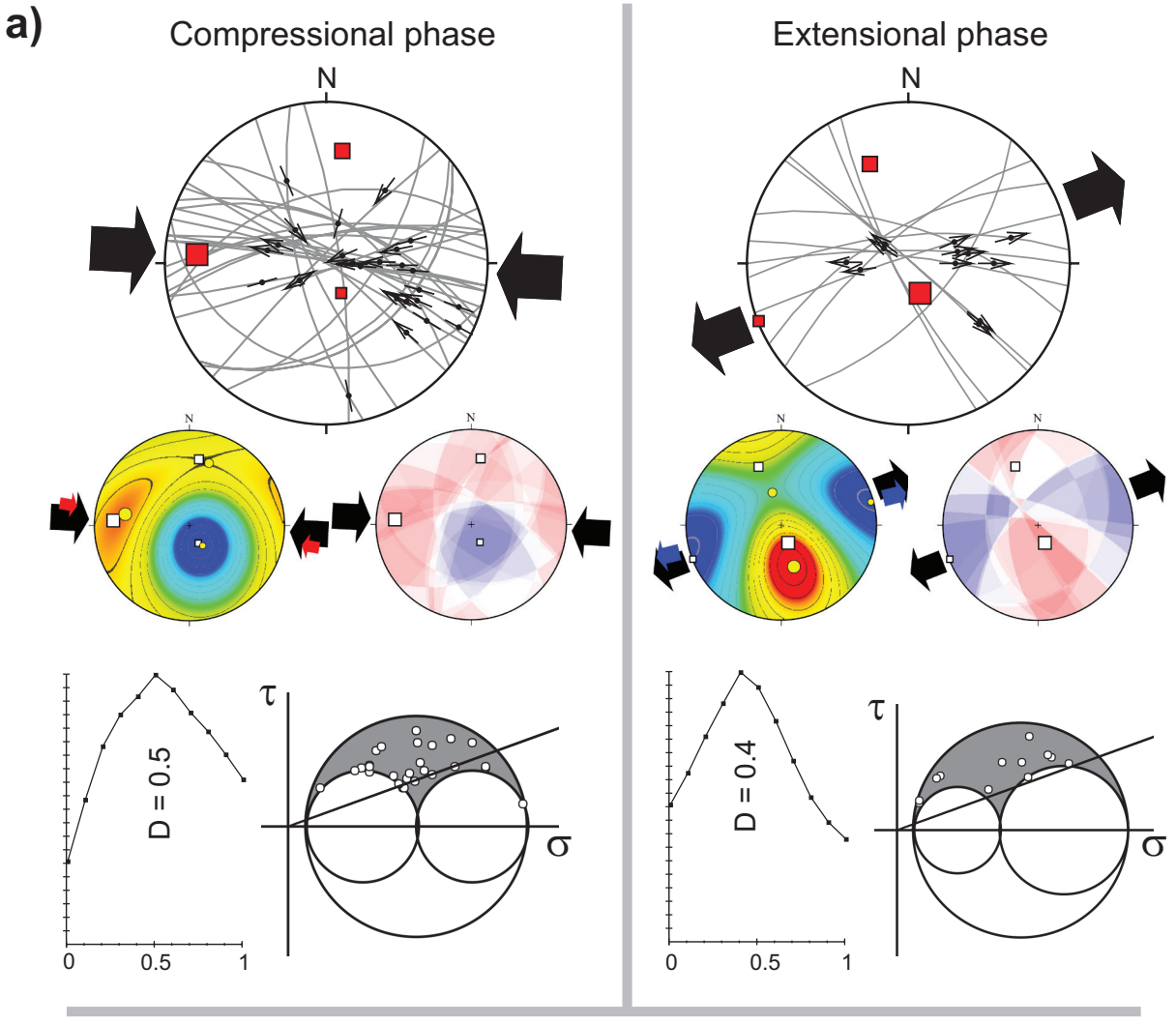
a)
Compressional phase
Extensional phase
N
D = 0.5
D = 0.4
τ
σ
0
0.5
1

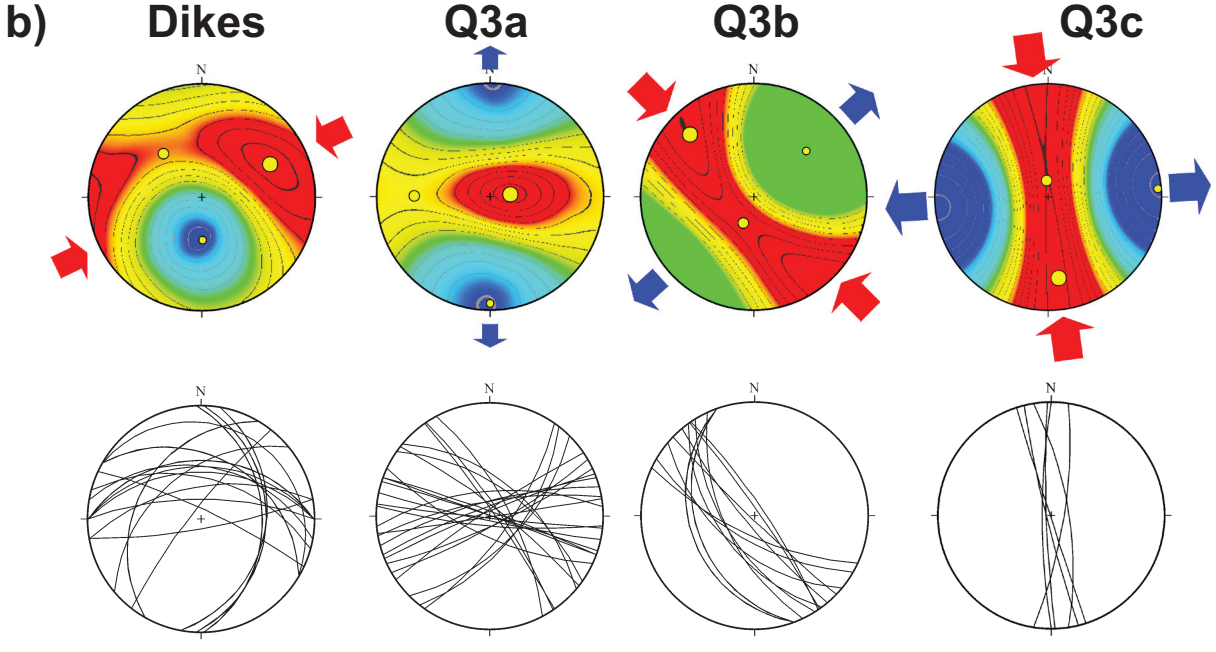
b)
Dikes
Q3a
Q3b
Q3c
N

in the separation of fault-slip data into two main groups with respect to the orientation of the paleostress axes (Fig. 9) and with respect to the stress ratio, represented by the D parameter, where $D = (\sigma_2–\sigma_3)/(\sigma_1–\sigma_3)$ and σ_1, σ_2, σ_3 are the maximum, intermediate, and minimum principal stresses.

8. Discussion

8.1. Paleostress analysis

Paleostress analysis of fault-slip data resulted in the identification of two stress phases (Fig. 9a), one corresponding to a compressional regime (subvertical σ_3) with σ_1 oriented WNW–ESE (i.e. subparallel to the Roudný "Main Vein") and the other corresponding to an extensional regime (subvertical σ_1) with subhorizontal NE–SW oriented σ_3. Validity of this analysis from the numerical Gauss method has been tested against the graphical Right Dihedra metod of Angelier and Mechler (1977). Paleostress analysis (Fig. 9b) of mode 1 (extension) fractures represented by "dikes" (aplite–pegmatite dikes and monomineral tourmaline veins) and quartz veins (Q3c) yielded similar stress orientation as fault-slip data (Fig. 9a). Two other subsets of quartz veins (Q3a and Q3b) do not match exactly the two above distinguished stress phases and possibly reflect local stress variations that occurred in between the two major phases.

Based on the similarity of stress tensors (Fig. 9a vs. Fig. 9b) we suggest formation of most of aplite–pegmatite dikes and monomineralic tourmaline veins during the compressional phase, while most of quartz veins originated probably during the extensional phase. Limited cross-cutting relationships indicate three successive substages of Q3 vein formation (Q3a, Q3b and Q3c) and support an idea of clockwise rotation of σ_3 paleostress axis orientation from N–S to E–W during their formation. Similar situation was documented at Hříva, an Ag–Pb–Zn bearing quartz stockwork located *c.* 5 km to the N from Roudný (Hübst et al. 2011; most quartz here veins exhibit orientation same as Q3b veins at Roudný). Formation of Q3b and Q3c veins is compatible with the strike-slip stress regime.

Finally, the existence of two (four) bilaterally symmetrical maxima of Q3a veinlets on stereograms (Fig. 7) may be explained by the dominance of an extensional component in the formation of Q3a veins striking WNW–ESE, while those striking ENE–WSW were formed under shear stress (resulting from a combination of extensional and compressional stress subhorizontal components).

As concerns the Roudný ore-body delimitating faults, the subvertical faults striking WNW–ESE (i.e. the "Main Vein" or the Hangingwall Fault) experienced net reverse faulting with only very limited fluid flow during the compressional phase. The opening (reactivation?) of the Roudný "Main Vein" fracture with the formation of massive quartz gangue (Q1, Q2; i.e. stage of main fluid flow) occurred during the onset of the extensional stage. The relatively limited length of the "Main Vein" (*c.* 100 m along the strike) supports its formation as a pure extension vein or as a hybrid extension–shear vein (suggesting minor rotation of σ_3 and σ_1 axes).

In contrast to paleostress analysis of Brandmayr et al. (1995), limited to the southernmost part of the Blanice Graben, we did not identify a strike-slip stress phase (subvertical σ_2; except for the orientation of Q3b and Q3c veins, see Fig. 9b). This may reflect either local differences in the stress distribution along a large-scale structure or, more probably, all the stress during the strike-slip phase was released along the major faults (i.e. border and central faults) of the Blanice Graben that have no outcrops in the studied area. Finally, similar orientation of the minimum stress axis (σ_3) of the strike-slip phase of Brandmayr (1995) and of our extensional phase advocates for gradual transition between these two phases. The brittle-tectonic evolution of the central part of the Blanice Graben can be thus separated into compressional, strike-slip and extensional stress phases (chronologically arranged).

8.2. Comments on the form of the Main Vein at the Roudný deposit

There are not many descriptions and schemes of the "Main Vein". Probably the most instructive ones are given by Šusta (1922; his tab. 2 and figs 6 and 7). The "Main Vein" is usually reported as an E–W or WNW–ESE striking single of variable thickness, locally split into several subparallel veins. When vein splitting is mentioned, the individual veins are usually located very close to each other (e.g. tab. 2 in Šusta 1922). They all merge into a single vein in schematic drafts like our Fig. 5.

During the data compilation for our summary (Fig. 5), we found a good correlation between the ore grade, the existing form/strike of the "Main Vein" and the grouping/distribution of the mined blocks. The mined blocks are frequently arranged in quasi-linear arrays that we interpret as a trend of the "Main Vein".

It is obvious from the summary (Fig. 5) that the "Main Vein" is straight and strikes WNW–ESE at the upper and deeper levels, whereas at the middle levels (–170 to –230 m) it is curviplanar, duplicated, and locally resembles two sigmoidal *en-echelon* tension veins (level –200 m).

The *en-echelon* local form of the "Main Vein" is not compatible with the general sinistral strike-slip regime along the Blanice Graben. It would require NNW–SSE oriented principal extension and sinistral shearing along the "Main Vein" (i.e. the opposite sense of movements than that associated with Riedel R' shears of the Blanice Graben). Therefore local reorientation of the stress field

must have occurred (accompanied by anticlockwise rotation of σ_1 and σ_3 stress axes by about 60° in a vertical segment delimitated by present mine levels –140 to –230 m). This could be indicated by the curved shape of the Michal and Pavlína faults, which exhibit large variations in their dip and/or strike. The stress field associated with non-planar faults, as well as near-to-fault terminations and/or at-fault intersections (e.g. Pollard et al. 1993; Nieto-Samaniego and Alaniz-Alvarez 1997; Nieto-Samaniego 1999; Gapais et al. 2000; Maniatis and Hampel 2008; Sperner and Zweigel 2010) can differ markedly from the regional stress field orientation. Finally, difference of about 60° was found in the density maxima of the S_1 poles ("mine surface" versus "mine underground"; Fig. 6a). All these factors could have played a role in the formation of the locally irregular shape of the "Main Vein".

8.3. Comparison of structural data from the Roudný mine with those from the Ratibořské Hory–Stará Vožice ore district

Vein type Ag–Pb–Zn deposits represent typical ore mineralization related to late Variscan to early post-Variscan evolution of the Blanice Graben. Among them, the Ratibořské Hory–Stará Vožice (RHSV) district is the most typical example. In addition, it is located only 20 km to the S of the Roudný mine and is therefore worth comparing.

Figure 10 summarizes orientation of non-mineralized and mineralized fault segments (inclusive ore veins) from the RHSV district along with data from the Roudný mine. The data for the RHSV district were extracted from the maps of Nouza (1988) and were processed in segments of 10 m length.

With respect to the general orientation of brittle fractures within a shear zone (e.g. Wilcox et al. 1973; Hodgson 1989), orientation of non-mineralized faults from the RHSV district correlates very well with the orientation of pressure shears (NNE–SSW oriented maximum) and with Riedel R' shears (WNW–ESE oriented faults). Joints at the Roudný deposit exhibit nearly the same orientation distribution. Therefore, we suggest that the NNE–SSW oriented joints at Roudný originated as pressure shears. In contrast to the RHSV district, the fault pattern at the Roudný deposit is dominated by the WNW–ESE and E–W oriented structures. The former most probably originated as Riedel R' shears, while the origin of the later is difficult to determine.

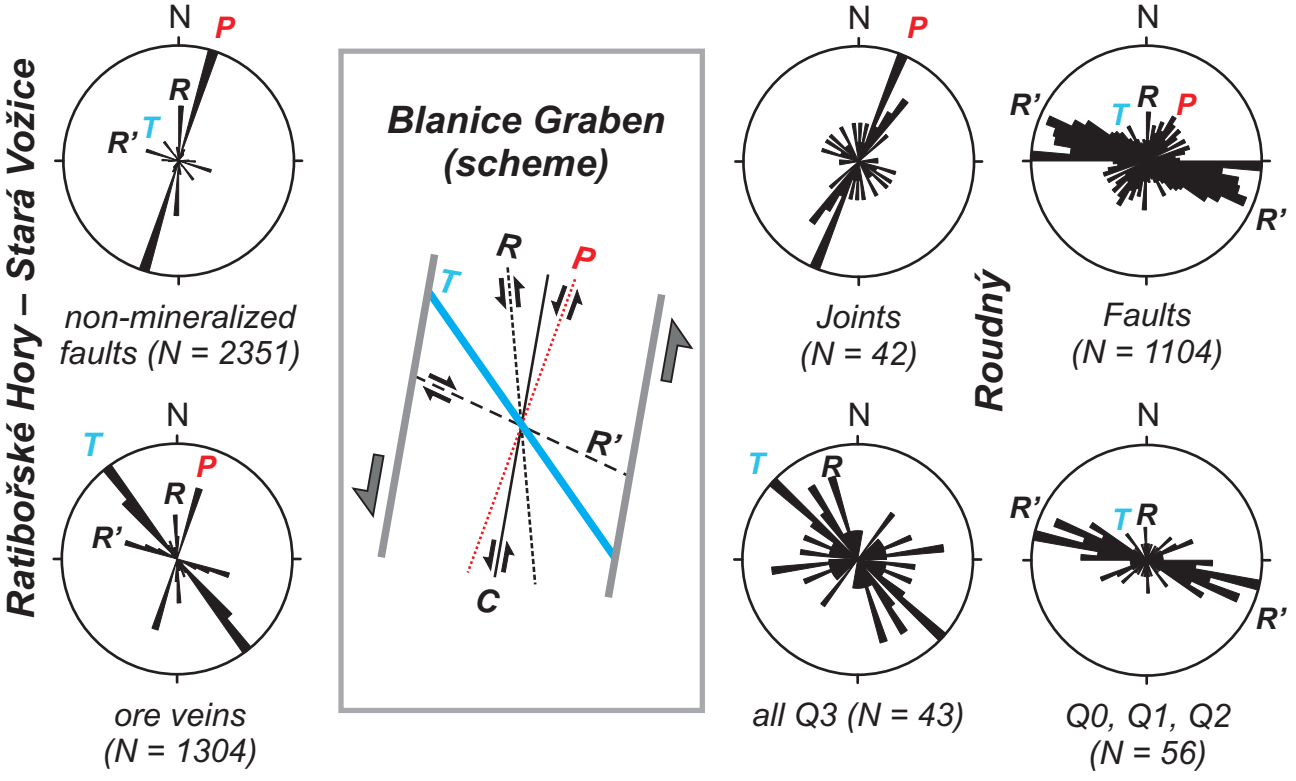

Fig. 10 Comparison of strikes of non-mineralized and mineralized faults (and veins) from the Ratibořské Hory–Stará Vožice Ag–Pb–Zn district with similar data and non-mineralized joints from the Roudný Au–Ag deposit. The Blanice Graben scheme depicts the general orientation of various types of fractures compatible within a sinistral shear zone (strike-slip zone). Strike maxima in Rose-type diagrams are labeled in similar way as in the scheme.

Most of the ore structures in the RHSV district represent typical extension veins (oriented at 45° to the strike of the Blanice Graben). The rest of them resemble Riedel R' shears and pressure shears, a few of them correlate with the orientation of Riedel R shears and central shears. The situation at the Roudný deposit is again quite different. The orientation of most of the early quartz veins (Q1, Q2) is compatible with that of Riedel R' shears (WNW–ESE), while the orientation of the late quartz veins (Q3) is compatible with extension fractures (NW–SE).

The orientation of major structures in both ore districts is thus compatible with the overall sinistral strike-slip model of the Blanice Graben. Differences between the abundance of individual vein/fracture types in individual ore districts reflect different timing and/or stress magnitudes.

9. Conclusions

Combined study of brittle to ductile structural elements at surface outcrops of the historical Roudný mine together with review of the existing geological information allowed us to reinterpret the form and the genesis of the Roudný ore body, as well as bring new light on the brittle-tectonic evolution of the central part of the Blanice Graben. Three stress phases were distinguished: compressional, strike-slip, and extensional (from the oldest to the youngest).

During a compressional phase with the principal shortening in the WNW–ESE direction, most of small aplite–pegmatite dikes/pockets formed (generally subparallel to the S_1 foliation), followed by fracture-related tourmalinization (i.e. monomineralic tourmaline veins). The main faults delimiting the Roudný ore body were also formed, or at least initiated, at this stage.

Major tectonic movements along the Blanice Graben probably occurred during the strike-slip phase. Unfortunately, there is poor evidence for this stage in the fault-slip data in the studied area. The orientation of fractures, joints and hydrothermal veins at the Au–Ag (Roudný) and Ag– Pb– Zn (Ratibořské Hory–Stará Vožice) ore districts/deposits, however, fits very well the sinistral strike-slip model of the Blanice Graben tectonic evolution. Mineralized early quartz veins (Q1, Q2) at Roudný were formed as tension or as mixed-mode, tension-shear (R' Riedel shear) fractures, followed by extensional Q3a veins. Most of the Ag–Pb–Zn-bearing veins at the Ratibořské Hory–Stará Vožice district represent typical tension fractures, oriented NW–SE. Orientation of most of Q3b veins at Roudný is compatible with this phase.

The strike-slip (or transtensional) regime then gradually evolved into pure extension regime with the E–W oriented principal extension. Regional hydrothermal fluid flow was still high, but it corresponded to its late phase. At the Roudný deposit, this phase is documented only by rare Q3c extension veins, correlative with numerous N–S trending barren quartz veins on a regional scale.

We interpret the "Main Vein" as well as the whole ore body at the Roudný deposit as an extension vein/fracture of limited extent along its strike, but of significant extent along its dip. Its formation was initiated as Riedel R' shear and later developed into a hybrid shear–extension mode. From the kinematic point of view, the Roudný deposit represents an integral part of the overall sinistral strike-slip evolution of the Blanice Graben.

Acknowledgements. This paper benefited from the financial support of the Grant Agency of Charles University (project No. 151810) and of Ministry of Education of the Czech Republic to the Faculty of Science, Charles University (project MSM 0021620855). We also greatly acknowledge the constructive reviews by J. Žalohar and one anonymous referee, and editorial comments of J. Žák and V. Janoušek.

References

Angelier J, Mechler P (1977) Sur une méthode graphique de recherche de constraintes principales également utilisable et en séismologie: la méthode des diédres droits. Bull Soc Géol France 19: 1309–1318

Bankwitz P, Bankwitz E, Thomas R, Wemmer K, Kämpf H (2004) Age and depth evidence for pre-exhumation joints in granite plutons: fracturing during the early cooling stage of felsic rock. In: Cosgrove JW, Engelder T (eds) The Initiation, Propagation and Arest of Joints and Other Fractures. Geological Society of London Special Publications 231: 25–47

Bernard JH (1991) Empirical types of ore mineralizations in the Bohemian Massif. Czech Geological Survey, Prague, pp 1–181

Bierlein FP, Crowe DE (2000) Phanerozoic orogenic lode gold deposits. In: Hagemann SG, Brown PE (eds) Gold in 2000. Reviews in Economic Geology 13: 103–139

Blenkinsop TG (2008) Relationships between faults, extension fractures and veins, and stress. J Struct Geol 30: 622–632

Bouchot V, Milési JP, Lescuyer JL, Ledru P (1997) Les minéralisations aurifères de la France dans leur cadre géologique autour de 300 Ma. Chron Rech Miniere 528: 13–62

Brandmayr M, Dallmeyer RD, Handler R, Wallbrecher E (1995) Conjugate shear zones in the Southern Bohemian Massif (Austria): implications for Variscan and Alpine tectonothermal activity. Tectonophysics 248: 97–116

Breiter K (2001) South Bohemian Pluton. Overview. In: Bankwitz P, Bankwitz E, Bahat D, Breiter K, Kämpf

H (eds) South Bohemian Pluton. Exkursionsführer und Veröffentlichungen der Gesellschaft für Geowissenschaften, Berlin, 212: 130–141

Breiter K, Sokol A (1997) Chemistry of the Bohemian granitoids: geotectonic and metallogenetic implications. Sbor geol Věd, ložisk Geol Mineral 31: 75–96

Cox SF (1999) Deformational controls on the dynamics of fluid flow in mesothermal gold systems. In: McCaffrey KJW, Lonergan L, Wilkinson JJ (eds) Fractures, Fluid Flow and Mineralization. Geological Society of London Special Publications 155: 123–140

Doblas M (1998) Slickenside kinematic indicators. Tectonophysics 295: 187–197

Dörr W, Zulauf G (2010) Elevator tectonics and orogenic collapse of a Tibetan-style plateau in the European Variscides: the role of the Bohemian shear zone. Int J Earth Sci (Geol Rundsch) 99: 299–325

Faryad SW, Nahodilová R, Dolejš D (2010) Incipient eclogite facies metamorphism in the Moldanubian granulites revealed by mineral inclusions in garnet. Lithos 144: 54–69

Fiala J (1995) General characteristics of the Moldanubian Zone. In: Dallmeyer RD, Franke W, Weber K (eds) Pre-Permian geology of Central and Eastern Europe. Springer-Verlag, Berlin, pp 417–418

Franke W (2000) The mid-European segment of the Variscides: tectonostratigraphic units, terrane boundaries and plate tectonic evolution. In: Franke W, Haak V, Oncken O, Tanner D (eds) Orogenic Processes: Quantification and Modelling in the Variscan Belt. Geological Society of London Special Publications 179: 35–61

Friedl G, Cooke RA, Finger F, McNaughton NJ, Fletcher IR (2011) Timing of Variscan HP–HT metamorphism in the Moldanubian Zone of the Bohemian Massif: U–Pb SHRIMP dating on multiply zoned zircons from a granulite from the Dunkelsteiner Wald Massif, Lower Austria. Mineral Petrol 102: 63–75

Gapais D, Cobbold PR, Bourgeois O, Rouby D, de Urreiztieta M (2000) Tectonic significance of fault-slip data. J Struct Geol 22: 881–888

Goldfarb RJ, Groves DI, Gardoll S (2001) Orogenic gold and geologic time: a global synthesis. Ore Geol Rev 18: 1–75

Hála M (1923) Modern gold mine: detailed discussion of dressing gold-bearing ores and of gold metallurgy. Naše hory a hutě – special edition, Kladno, 1–19 (in Czech)

Hodgson CJ (1989) The structure of shear-related, vein-type gold deposits: a review. Ore Geol Rev 4: 231–273

Holub FV, Klečka M, Matějka D (1995) Igneous activity. In: Dallmeyer RD, Franke W, Weber K (eds) Pre-Permian Geology of Central and Eastern Europe. Springer-Verlag, Berlin, pp 444–452

Holub FV, Cocherie A, Rossi P (1997a) Radiometric dating of granitic rocks from the Central Bohemian Plutonic Complex (Czech Republic), constraints on the chronology of thermal and tectonic events along the Moldanubian–Barrandian boundary. C R Acad Sci Paris Earth Planet Sci 325: 19–26

Holub FV, Machart J, Manová M (1997b) The Central Bohemian Plutonic Complex: geology, chemical composition and genetic interpretation. Sbor geol Věd, ložisk Geol Mineral 31: 27–50

Holub V (2001) The occurrences of the Permo–Carboniferous sequences in the Blanice Graben. In: Pešek J, Holub V, Jaroš J, Malý L, Martínek K, Prouza V, Spudil J, Tásler R (eds) Geology and Deposits of Upper Paleozoic Limnic Basins of the Czech Republic. Czech Geological Survey, Prague, pp 197–207 (in Czech)

Hradecký F (1911a) Gold mine at Roudný (part I). Hornické a hutnické listy 10: 146–148 (in Czech)

Hradecký F (1911b) Gold mine at Roudný (part II). Hornické a hutnické listy 12: 175–178 (in Czech)

Hübst Z, Zachariáš J, Selmi M (2011) Silver-bearing stringer at Hříva near Louňovice pod Blaníkem: structural and fluid evolution. Sbor Jihočes Muz v Čes Budějovicích, Přír vědy 51: 43–56 (in Czech)

Janoušek V, Gerdes A (2003) Timing the magmatic activity within the Central Bohemian Pluton, Czech Republic: conventional U–Pb ages for the Sázava and Tábor intrusions and their geotectonic significance. J Czech Geol Soc 48: 70–71

Janoušek V, Rogers G, Bowes DR (1995) Sr–Nd isotopic constraints on the petrogenesis of the Central Bohemian Pluton, Czech Republic. Geol Rundsch 84: 520–534

Janoušek V, Braithwaite CJR, Bowes DR, Gerdes A (2004) Magma-mixing in the genesis of Hercynian calc-alkaline granitoids: an integrated petrographic and geochemical study of the Sázava intrusion, Central Bohemian Pluton, Czech Republic. Lithos 78: 67–99

Janoušek V, Wiegand B, Žák J (2010) Dating the onset of Variscan crustal exhumation in the core of the Bohemian Massif: new U–Pb single zircon ages from the high-K calc-alkaline granodiorites of the Blatná suite, Central Bohemian Plutonic Complex. J Geol Soc London 167: 347–360

Ježek B (1930) Expert geological report on the gold mine at Roudný. Unpublished document of The "Vysoká škola baňská v Příbrami" (stored at Geofond ČR; P013019), pp 1–40 (in Czech)

Ježek B (1931) About current conditions and prospects for the gold mine at Roudný. Báňský svět 10: 1–5 (in Czech)

Ježek B, Hoffman AO (1933) Gold mine at Roudný. Báňský svět 12: 85–93, 100–107, 115–118, 126–132 (in Czech)

Klečka M, Matějka D (1996) Moldanubian Batholith – an example of the evolution of the Late Paleozoic granitoid magmatism in the Moldanubian Zone, Bohemian Massif (Central Europe). In: Srivastava RK, Chandra R (eds) Magmatism in Relation to Diverse Tectonic

Settings. Oxford and IBH Publishing Co., New Delhi, pp 353–373

Komínek E, Blüml A, Drozen J, Hájek J, Horáková M, Procházka J (1990) Exploration for Au–W ores – Roudný. Unpublished report of Geoindustria Jihlava (stored at Geofond ČR; P76710), pp 1–60 (in Czech)

Košler J, Kelley SP, Vrána S (2001) $^{40}Ar/^{39}Ar$ hornblende dating of a microgranodiorite dyke: implications for early Permian extension in the Moldanubian Zone of the Bohemian Massif. Int J Earth Sci (Geol Rundsch) 90: 379–385

Kovald (1951) Schematic map and profile of ore veins at the Barbora adit at Roudný. Unpublished internal report (stored at Geofond ČR; P4932), pp 1–3 (in Czech)

Malachov A (1954) Annual report (1953) – prospecting at Roudný. Unpublished internal report of the Západočeský rudný průzkum (stored at Geofond ČR; P4828), pp 1–3 (in Czech)

Maniatis G, Hampel A (2008) Along-strike variations of the slip direction on normal faults: insights from three-dimensional finite-element models. J Struct Geol 30: 21–28

Matějka D, Janoušek V (1998) Whole-rock geochemistry and petrogenesis of granites from the northern part of the Moldanubian Batholith (Czech Republic). Acta Univ Carol, Geol 42: 73–79

Micklethwaite S, Sheldon HA, Baker T (2010) Active fault and shear processes and their implications for mineral deposits formation and discovery. J Struct Geol 32: 151–165

Morávek P, Aichler J, Doškář Z, Duda J, Ďurišová J, Hauk J, Janatka J, Kalenda Z, Klomínský J, Květoň P, Litochleb J, Malec J, Mrázek I, Novák F, Pouba Z, Pudilová M, Punčochář M, Skácel J, Soukup B, Studničná B, Sztacho P, Šponar P, Tásler R, Váňa T, Vaněček M, Veselý J (1992) Gold in the Bohemian Massif. Czech Geological Survey, Prague, pp 1–245 (in Czech with extensive English summary).

Nieto-Samaniego AF (1999) Stress, strain and fault patterns. J Struct Geol 21: 1065–1070

Nieto-Samaniego AF, Alaniz-Alvarez SA (1997) Origin and tectonic interpretation of multiple fault patterns. Tectonophysics 270: 197–206

Nouza R (1988) Prognostic evaluation of Ag–Pb–Zn mineralizations of the Blanice Furrow. Unpublished Ph.D. thesis, Faculty of Science, Charles University in Prague, pp 1– 143 (in Czech)

Novák M (1956) Mineralogy and petrology of ores from Roudný. Unpublished internal report of the Ústav pro výzkum rud (stored at Geofond ČR; P6001), pp 1–43 (in Czech)

Paterová B (2001) Mineralogical and geochemical study of the Roudný near Vlašim deposit. Unpublished M.Sc. Thesis, Faculty of Science, Charles University in Prague, pp 1– 85 (in Czech)

Pollard DD, Saltzer SD, Rubin AM (1993) Stress inversion methods: are they based on faulty assumptions? J Struct Geol 15: 1045–1054

Sibson RH (2000) Fluid involvement in normal faulting. J Geodyn 29: 469–499

Slavík F (1912) Roudný. Sborník klubu přírodovědného v Praze 1: 127–150 (in Czech)

Sperner B, Zweigel P (2010) A plea for more caution in fault-slip analysis. Tectonophysics 482: 29–41

Šusta V (1922) Gold mine Roudný. Knihovna Státního geologického Ústavu Československé Republiky, Prague, 4: 1–32 (in Czech)

Švestka J, Hron M (1993) Final report: gold placers. Prospecting stage. Unpublished report of the GMS a.s. company (stored at Geofond ČR; FZ006471), pp 1–196 (in Czech)

Urban K (1954) Annual report Roudný. Unpublished internal report of the Západočeský rudný průzkum (stored at Geofond ČR; P6698), pp 1–5 (in Czech)

Urban K (1956) Final report (1955) – Roudný: Roudný section. Unpublished internal report of the Západočeský rudný průzkum (stored at Geofond ČR; P7587), pp 1–8 (in Czech)

Urban K (1957) Final report (1956) – Roudný: Roudný section. Unpublished internal report of the Západočeský rudný průzkum (stored at Geofond ČR; P8687), pp 1–32 (in Czech)

Vrána S, Bártek J (2005) Retrograde metamorphism in a regional shear zone and related chemical changes: the Kaplice Unit of muscovite–biotite gneisses in the Moldanubian Zone of southern Bohemia, Czech Republic. J Czech Geol Soc 50: 43–57

Vrána S, Slabý J, Bendl J (2005) The Kaplice dyke swarm of biotite granodiorite porphyry and its relationship to the Freistadt granodiorite, Moldanubian Batholith. J Czech Geol Soc 50: 9–17

Wilcox RE, Harding TP, Seely DR (1973) Basic wrench fault tectonics. Bull Am Assoc Pet Geol 57: 57–96

Zachariáš J, Stein H (2001) Re–Os ages of Variscan hydrothermal gold mineralisations, Central Bohemian metallogenetic zone, Czech Republic. In: Piestrzyński et al. (eds) Mineral Deposits at the Beginning of the 21st Century. Swets & Zeitlinger Publishers, Lisse, pp 851–854

Zachariáš J, Pertold Z, Pudilová M, Žák K, Pertoldová J, Stein H, Markey R (2001) Geology and genesis of Variscan porphyry-style gold mineralization, Petráčkova hora deposit, Bohemian Massif, Czech Republic. Miner Depos 36: 517–541

Zachariáš J, Frýda J, Paterová B, Mihaljevič M (2004) Arsenopyrite and As-bearing pyrite from the Roudný deposit, Bohemian Massif. Mineral Mag 68: 31–46

Zachariáš J, Paterová B, Pudilová M (2009) Mineralogy, fluid inclusion, and stable isotope constraints on the gen-

esis of the Roudný Au–Ag deposit, Bohemian Massif. Econ Geol 104: 53–72

Zemek V (2001) Historical gold mine Roudný. Podblanické ekocentrum ČSOP a Muzeum okresu Benešov, Vlašim, pp 1–108 (in Czech, an appendix of a quarterly review 'Pod Blaníkem', vol. 5 (28))

Zoubek V (1945) Geological opinion on the condition of the gold-bearing deposit at Roudný. Unpublished internal report of the State Geological Institute of the Czechoslovak Republic (stored at Geofond ČR; P209), pp 1–4 (in Czech)

Žák J, Holub FV, Verner K (2005) Tectonic evolution of a continental magmatic arc from transpression in the upper crust to exhumation of mid-crustal orogenic root recorded by episodically emplaced plutons: the Central Bohemian Plutonic Complex (Bohemian Massif). Int J Earth Sci (Geol Rundsch) 94: 385–400

Žák J, Verner K, Holub FV, Kabele P, Chlupáčová M, Halodová P (2012) Magmatic to solid state fabrics in syntectonic granitoids recording early Carboniferous orogenic collapse in the Bohemian Massif. J Struct Geol 36: 27–42

Žák K, Vlašímský P, Snee LW (1998) ^{40}Ar–^{39}Ar cooling ages of selected rocks of the Příbram ore region and the question of timing of sulphidic hydrothermal mineralization. Zpr geol výzk v r 1997: 172–173 (in Czech)

Žalohar J, Vrabec M (2007) Paleostress analysis of heterogeneous fault-slip data: the Gauss method. J Struct Geol 29: 1798–1810